Cloud variability as revealed in outgoing infrared spectra: Comparing model to observation with spectral EOF analysis

Xianglei Huang,[1] John Farrara,[2] Stephen S. Leroy,[3] Yuk L. Yung,[1] and Richard M. Goody[4]

Received 3 October 2001; revised 8 January 2002; accepted 16 January 2002; published 30 April 2002.

[1] Spectrally resolved outgoing radiance is a potentially powerful tool for testing climate models. To show how it can be used to evaluate the simulation of cloud variability, which is the principal uncertainty in current climate models, we apply spectral empirical orthogonal function (EOF) analysis to satellite radiance spectra and synthetic spectra derived from a general circulation model (GCM). We show that proper averaging over a correct timescale is necessary before applying spectral EOF analysis. This study focuses on the Central Pacific and the western Pacific Warm Pool. For both observation and GCM output, cloud variability is the dominant contributor to the first principal component that accounts for more than 95% of the total variance. However, the amplitude of the first principal component derived from the observations ($2 \sim 3.4$ W m^{-2}) is $2 \sim 6$ times greater than that of the GCM simulation. This suggests that cloud variability in the GCM is significantly smaller than that in the real atmosphere. *INDEX TERMS:* 3359 Meterology and Atmospheric Dynamics: Radiative processes; 3360 Meterology and Atmospheric Dynamics: Remote sensing; 3337 Meterology and Atmospheric Dynamics: Numerical modeling and data assimilation; 3399 Meterology and Atmospheric Dynamics: General or miscellaneous

1. Introduction

[2] It is well known that clouds are the principal source of uncertainty in current climate models [*Cess et al.*, 1995]. The climate sensitivity, which is defined as the surface temperature increase caused by a doubling of CO_2, is strongly dependent on the cloud feedback [*Houghton et al.*, 2001]. Therefore, realistic cloud simulation is essential for reducing uncertainties in climate prediction. A widely used approach to evaluating cloud simulations is to compare simulated mean cloudiness with its observed counterpart. However, there is another meaningful way to evaluate model performance by studying the second-order statistics [*Leith*, 1975; *Bell*, 1980; *North et al.*, 1993; *Goody et al.*, 1998]. *Haskins et al.* [1997, 1999] clearly showed the power of spectrally resolved outgoing radiance for comparison of second and higher order statistics. Due to the lack of access to cloud data in models, work of *Haskins et al.* [1997, 1999] focused only on clear-sky situations. However, clouds are prominent components in the climate system and thus the information in cloudy spectra should not be overlooked. In this paper, we include both clear-sky and cloudy data in our study and apply the spectral empirical orthogonal function (EOF) analysis to spectrally resolved outgoing radiance. The methodology and results pertaining to clouds in the tropical atmosphere are discussed.

2. Data and Methodology

2.1. Observation

[3] The dataset of spectrally resolved radiance we used is the Infrared Interferometer Spectrometer (IRIS). It was a Michelson Fourier transform spectrometer flown from April 1970 to January 1971 on Nimbus 4. The corresponding ENSO phase during this period is moderate La Niña. It covered the spectral region from 400 to 1600 cm^{-1} with an apodized resolution of 2.8 cm^{-1}. The signal to noise ratio at the mid-point of the spectrum was better than 100 and degraded to about 20 at the frequency endpoints. IRIS was a nadir sounder with a field of view of about 95 by 120 km [*Hanel et al.*, 1972]. Its orbit was a sun-synchronous orbit at approximately 1100-km altitude, crossing the equator at around 0 and 12 hour local time. During the 10-month operational period, IRIS collected about 700,000 spectra.

[4] Our analysis is limited by the length of the observational record. We have only 10 months of observation from IRIS. Therefore, any climate processes with a characteristic timescales longer than 10 months is not addressed in this study. However, if we treat the atmosphere as an isolated system, most intrinsic time scales are shorter than one year. Some important but still poorly understood processes, such as the lifecycle of clouds, have timescales of less than several days. Therefore, the IRIS data are sufficiently long to test such physical processes in the model.

2.2. GCM and MODTRAN

[5] The UCLA GCM we work with is a recognized grid point model of the global atmosphere extending from the surface of the Earth to a height of 50 km [*Mechoso et al.*, 2000]. The horizontal resolution is $4° \times 5°$ in latitude and longitude. There are 9 layers in the troposphere and 6 layers in the stratosphere. The output is twice per day, at 0000 GMT and 1200 GMT. Cloud optical depth is computed based on liquid water and ice particle concentrations. A prediction scheme for cloud liquid water and ice based on a five-phase bulk microphysics is used [*Kohler*, 1999]. The GCM is forced with monthly averaged SST for the same period as IRIS. After we obtain the tropospheric vertical profiles of temperature, water vapor and cloud optical depth at each grid point from GCM, we input them into a radiative transfer model to calculate the outgoing spectrum at the top of the atmosphere at each grid point. Therefore, we have two spectra every day at each grid point.

[6] The radiative transfer model that we use is the MODTRAN 4.0 (MODerate resolution TRANsmittance code) developed by the Air Force Research Laboratory, with the capability of simulating the radiative effects of different kinds of clouds [*Wang and Anderson*, 1996]. It is well known that infrared radiation is strongly absorbed by optically thick clouds and the effect of scattering is secondary. *Cotton and Anthes* [1989] indicates that 90% of incident infrared radiation can be absorbed in less than 50-m pathlengths in a liquid cloud. This justifies simulating cloud

[1]Division of Geological and Planetary Sciences, California Institute of Technology, USA.
[2]Department of Atmospheric Sciences, University of California at Los Angeles, USA.
[3]Earth and Space Sciences Division, Jet Propulsion Laboratory, California Institute of Technology, USA.
[4]Department of Chemistry and Chemical Biology, Harvard University, USA.

0094-8276/02/2001GL014176

radiative behavior as simply absorptive rather than as multiple scattering, a convenience we desire considering the computational expense which would otherwise be involved in generating multiple scattering computations for ~80,000 spectra. The detailed discussion of the feasibility of using MODTRAN in such comparisons can be found in *Haskins et al.* [1997].

[7] Tropospheric profiles are taken from the model output while stratospheric profiles are taken from standard profiles used by MODTRAN. The reasons for doing this are: (1) it is difficult to avoid spurious reflection of upward-propagating waves in a model with a rigid upper boundary at 50 km [*Callaghan et al.*, 1999; *Salby, private communication*]; (2) the 6-layer representation of the stratosphere in the model might not be enough for a satisfactory simulation of the stratospheric variability. As a result of (1) and (2), the variability in the stratosphere is less realistic. Therefore, we eliminate stratospheric variability so that we can focus on the troposphere.

2.3. Data Manipulation

[8] Before we can carry out our spectral EOF analysis, we need to average the spectra over certain regions and time scales. This is necessary because the spatial and temporal sampling patterns of observations are not the same as those in the model. In this study, we focus on two regions. One is the Central Pacific, defined as 180°W to 130°W and 10°S to 10°N; the other is the Warm Pool, defined as 90°E to 150°E and 10°S to 10°N. During its 10-month flight, IRIS collected 10804 spectra over the Central Pacific and 8467 spectra over the Warm Pool. For the GCM we use, there are 66 grid points in the Central Pacific and 78 grid points in the Warm Pool. The appropriate timescale for the averaging is discussed in the next paragraph. For IRIS data, the number of spectra collected during the ascending node is different from those collected during the descending node. Before we average the data, we weight data from the ascending branch and from the descending branch such that day-night contrasts are eliminated.

[9] We are forced to choose a temporal averaging window suitably long to reduce complications arising from undersampling by the sounder, a problem typical of any sounder sensitive to clouds [*Salby*, 1989]. The asynoptic nature of satellite measurements is especially important for clouds because the space and time scales of cloud variability are easily less than that of the sampling. *Salby* [1989] pointed out that clouds change typically in hours, which is much shorter than the time for the globe to be covered by the satellite and that a sufficiently long period averaging can remove the aliasing from unresolved random variability. We estimate the timescale to do the average with synthetic spectra based on GCM output. We use two different ways to get the daily average over a given region. One is to do average with all grid points inside this region (hereafter, "average-all" method), the other is to find the grid points nearest to the satellite tracks and average spectra only at those grid points (hereafter, "track-orbit" method). Obviously, the latter method is more directly suitable for comparison to IRIS spectra. With these two methods, we obtain the averages over periods longer than one day. When the averaging is done over a long enough timescale, the difference of two sets of averaged spectra should be very small, demonstrating that the "track-orbit" method is already a good approximation to the 'average-all' method at this timescale. Figure 1 shows a comparison of the standard deviation of these two sets of spectra over the Central Pacific. It can be seen that for 5-day averaging the standard deviation from the "average-all" method is only half of that from the "track-orbit" method; when the averaging period is 25 days, they are almost the same. Therefore, for the Central Pacific, we adopt 25-day averages. We apply the same analysis to the Warm Pool and it shows 25 days is also long enough for discrepancies in standard deviation to cancel.

2.4. Spectral EOF Analysis

[10] We perform spectral EOF analysis on the spectra obtained as described in 2.3. Given a set of radiances measured at

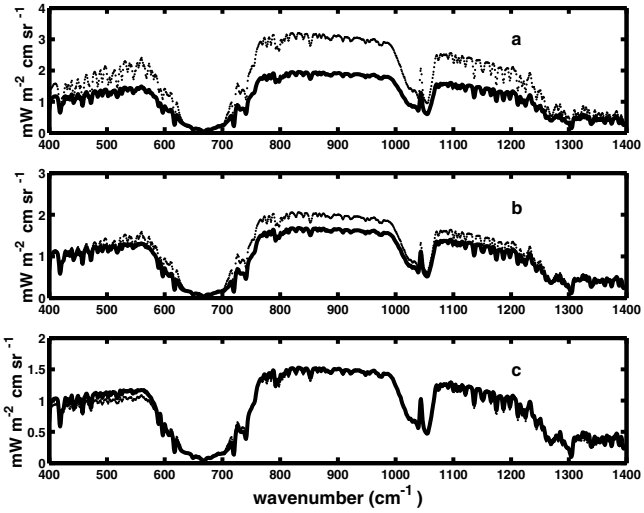

Figure 1. (a) The standard deviation of spectrally resolved radiance derived from the GCM. The dotted line was computed from data averaged over 5 days for the Central Pacific using the "track-orbit" method (as defined in the text). The solid line is the same as the dashed line, except that the averaging was performed using the 'average-all' method (as defined in the text). (b) Same as (a), except that the time interval for averaging is 20 days. (c) Same as (a), except that the averaging time is 25 days.

frequency ν, denoted as $I_\nu(t)$, the EOFs, $\phi_\nu^{(i)}$, are unit eigenvectors of covariance matrix

$$C_{\nu_1\nu_2} = \overline{\left(I_{\nu_1}(t) - \bar{I}_{\nu_1}\right)\left(I_{\nu_2}(t) - \bar{I}_{\nu_2}\right)} \quad (1)$$

where the overbar represents an average over all samples. Let λ_i be the eigenvalue corresponding to the i-th eigenvector $\phi_\nu^{(i)}$; then the *principal component* (PC) can be defined as

$$PC_\nu^{(i)} = \sqrt{\lambda_i}\phi_\nu^{(i)} \quad (2)$$

PCs have dimensions of radiance, so can be more easily interpreted than EOFs [*Haskins et al.*, 1999]. Compared with the spatial EOF analysis that is most widely used in the atmospheric sciences, this EOF analysis just replaces space with frequency.

[11] Principal components and covariance matrices are conjugates of each other. To compare EOFs of climate variables from observations and model is equivalent to comparing their second-order statistics. Moreover, the leading EOFs usually can be interpreted physically.

3. Results

[12] Figure 2(a) shows a comparison of the mean spectra over the Central Pacific obtained from IRIS observations and the MODTRAN calculations based on the GCM output. Figure 2(b) is the same as Figure 2(a), but for the Warm Pool. It can be seen that the differences between the observations and the model over the Central Pacific are much bigger than over the Warm Pool. For the Central Pacific, in the window region (800–1000 cm^{-1}), the brightness temperature of IRIS mean spectra is higher than that of the simulated mean spectra by more than 10 K. Since the window region is transparent to thermal radiance and the observed sea surface temperature is provided as a boundary condition for the model, this difference in the window region is most likely caused by clouds. In other words, on the average, the model has more clouds in the Central Pacific than the real atmosphere. The bright-

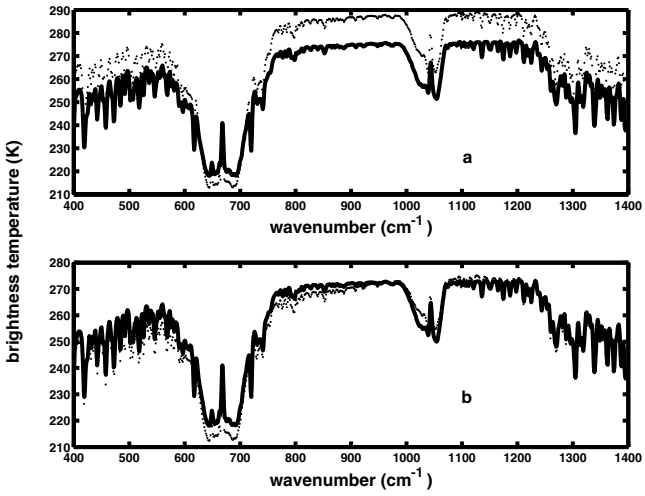

Figure 2. (a) The 10-month averaged radiance spectra over the Central Pacific. The dotted line is derived from IRIS observations, and the solid line is computed from the GCM. (b) The same as (a) for the Warm Pool.

ness temperature difference in the window region over the Warm Pool is less than 5 K.

[13] The comparison in the previous paragraph only shows how well the model simulates the atmosphere in the long-term mean state. It does not show how well the variability of model clouds matches that of the observations, and this is exactly what the spectral EOF analysis can tell us. Figure 3 presents the first *principal component* (hereafter, PC1) of the 25-day averaged spectra over the Central Pacific from IRIS and model data. Each PC1 explains the bulk of the variance: PC1 from IRIS accounts for 98.0% of the total variance, and that from the model also accounts for 98.0% of the total variance. The most striking difference is in the amplitudes of the PC1s. The peak of PC1 from IRIS in the window region is 3.5 mW m^{-2} cm str^{-1} (corresponding brightness temperature, hereafter T_B, is 2.4 K), while the counterpart from the model is only 1.5 mW m^{-2} cm str^{-1} (T_B = 1.2 K). The integral from 400 to 1400 cm^{-1} for IRIS PC1 is 2.05 W m^{-2}. For the model PC1, it is 0.88 W m^{-2}, less than half of the observed PC1. Given that both model and observed PC1 account for 98% of the

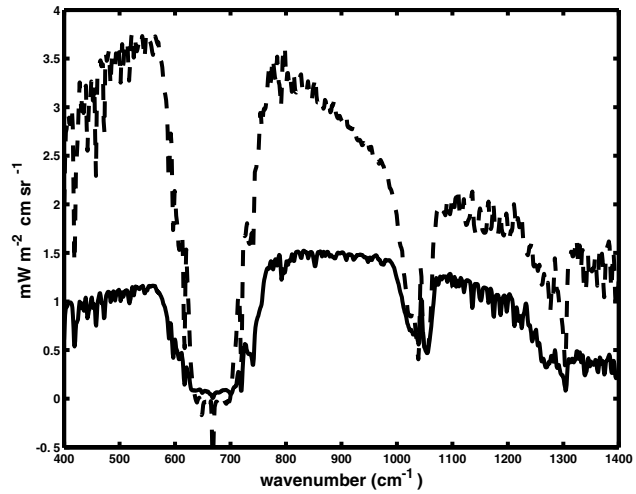

Figure 3. Comparison of the PC1 derived from 25-day averaged spectra over the Central Pacific from IRIS observations (dashed line) with that from the GCM.

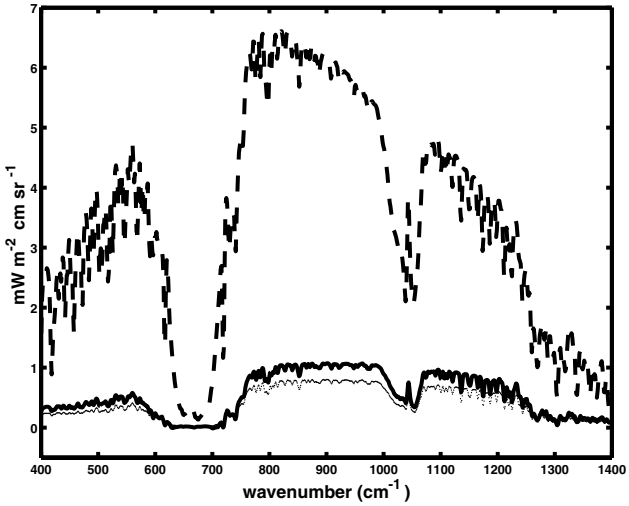

Figure 4. Comparison of the PC1 derived from 25-day averaged spectra over the Warm Pool from IRIS observations (dashed line) with that from the GCM (solid line). The dotted line is same as the solid line, except that the clouds have been interpolated to the value of local noon/midnight (refer to text for details).

total variance, this implies that, for the Central Pacific, the model variance in outgoing radiation is only about half of what we observed from IRIS. Figure 4 shows the observed and modeled PC1 for the Warm Pool. As in the case of the Central Pacific, PC1 explains most of the variance: for IRIS it accounts for 99.1% of the total variance and for the model 94.5%. The difference in amplitude is even larger than in the case of the Central Pacific. The peak of PC1 from IRIS in the window region is 6.6 mW m^{-2} cm str^{-1} (T_B = 4.8 K), while the counterpart from the model is only 1.1 mW m^{-2} cm str^{-1} (T_B = 0.96 K). The 400 to 1400 cm^{-1} integral for PC1 from IRIS is 3.4 W m^{-2}, and for PC1 from the model, it is 0.54 W m^{-2}. The model PC1 is only about one-sixth of the observed PC1 in this case. Since PC1 also explains almost all the variance for the Warm Pool, the model variance in the outgoing radiation is only about one-sixth of what was observed by IRIS.

[14] We apply a simple inversion scheme to explore the contribution of clouds to PC1. The detailed description of this scheme can be found in *Haskins et al.* [1999]. Simply put, stepwise regression is applied to each PC1 to determine the cloud contributions. There are four types of clouds in this scheme, the tops of which are located at 4, 8, 12 and 16 km. For each PC1, the amount of variance that can be explained by clouds is listed in Table 1. Except for the IRIS PC1 over the Central Pacific, clouds can explain on the order of 90% of the variance in all PC1s. The corresponding cloud height and cloud fraction change derived from this inversion scheme are also listed in Table 1. The results suggest that the most likely contributors to PC1s are high clouds rather than low clouds. They also suggest that the corresponding cloud heights derived from IRIS PC1s are higher than those from model, indicating that there might not be enough high cloud in the model.

Table 1. Summary of the Fraction of Variance of the PC1s Explained by Clouds, and the Corresponding Cloud Height and Cloud Fraction Change[a]

	Central Pacific		Warm Pool	
	IRIS	Model	IRIS	Model
Variance explained by cloud	70%	91%	99%	96%
Corresponding top of cloud	16km	12km	12km	8km
Corresponding cloud fraction change	2.9%	1.7%	7%	1.7%

[a] All these are derived from the inversion scheme mentioned in text.

Given the simplicity of the inversion scheme that we use, and the difficulties of the retrieval of infrared spectra under a cloudy situation, the results from this simple inversion may not be quantitatively robust. But qualitatively, it shows that the major contribution to PC1 is due to cloud. This is true for both IRIS observation and the GCM.

[15] Other than random fluctuations which can be smoothed out by averaging over a long period, there is another kind of temporal variability which we must take into account: diurnal variability. IRIS always sampled at local noon and midnight, but the GCM gave output at 1200 and 0000 GMT. So we need to investigate to what extent the two different time-sampling patterns affect the PC1. To tackle this issue, we do a simple test. We assume the cloud diurnal variations are sinusoidal, $C(t) = C_0 + C_a \sin[2\pi(t - T_m)/24]$, where C_0 is a constant term, and $0 \leq t \leq 24$ hour. The phase information is obtained from Bergman and Salby's studies about diurnal variations of cloud cover [*Bergman and Salby*, 1996]: for low cloud, $T_m \approx -2$; for high cloud, $T_m \approx 11$. Based on this sinusoidal curve, we can interpolate GCM cloud output to local noon and midnight. With these new cloud data, we can calculate spectra and do spectral EOF analysis. The dotted line in Figure 4 is the PC1 over the Warm Pool computed in this way. It can be seen that there is only a slight difference between this PC1 and the original PC1 (the solid line in Figure 4). Also *Bergman and Salby* [1996, 1997] show that diurnal variations of cloud over tropical ocean regions are weaker than those over landmasses, and the cloud diurnal contributions to the time-mean thermal flux are usually less than 1 W m^{-2}. Therefore, we conclude that although diurnal variations can bias our comparison results somewhat, it cannot explain the substantial difference found between the GCM and observations.

4. Conclusion

[16] The above sections clearly show that spectral EOF analysis can be a useful tool for comparing the second-order statistics of climate models and observations, even when clouds are included. After sampling problems are carefully treated, we demonstrate the discrepancy between observations and a selected climate model (the UCLA GCM) in the variability of outgoing infrared radiance. For the two regions that we study, cloud accounts for the vast majority of the variability in outgoing infrared radiance. However, the model underestimates the amplitude of cloud variations by a factor of 2∼6.

[17] It is a very interesting question where the underestimation of clouds in the model comes from. It could be related to an incorrect representation of the tropical low-frequency variability in the GCM, especially the intraseasonal variability. It is well known that the current GCMs cannot realistically simulate intraseasonal variability [*Slingo et al.*, 1996]. The dominant mode of tropical intraseasonal variability is the Madden-Julian Oscillation (MJO) [*Madden and Julian*, 1971], which is closely related to convective anomalies in the eastern hemisphere. This possibility is supported by the time series of 25-day running mean of the brightness temperature in the window regions. For the Warm Pool where one end of the MJO convective dipole is located [*Matthews*, 2000], the time series from IRIS shows clear peaks separated by approximately 50 days, which is close to the period of MJO. The time series from UCLA also shows intraseasonal oscillation, but the oscillation is much broader and the amplitude of oscillation is much smaller than that from IRIS. On the other hand, it is also possible that the deficiencies of the cloud parameterization scheme in the model also contribute to this underestimation.

[18] In summary, spectrally resolved radiance provides us an independent source for evaluating climate models. Compared with the traditional way of validating models by comparing thermodynamical variables, such as temperature and pressure, this approach is more comprehensive and more directly related to clouds. Moreover, the spectra and relevant statistics can disclose more information about clouds, such as the cloud height and cloud fraction change. This can provide useful diagnostics and insights for improving climate models.

[19] **Acknowledgments.** We thank A. Ingersoll, M. Gerstell, G. Toon and R. Zurek for valuable comments. We wish to thank two anonymous referees for improving the paper. This research is supported by NOAA grant Grant No. NA06EC0505 to the California Institute of Technology.

References

Bell, T. L., Climate sensitivity from fluctuation-dissipation: Some simple model tests, *Journal of Atmospheric Science*, *37*, 1700–1707, 1980.

Bergman, J. W., and M. L. Salby, Diurnal variations of cloud cover and their relationship to climatological conditions, *Journal of Climate*, *9*, 2802–2820, 1996.

Bergman, J. W., and M. L. Salby, The role of cloud diurnal variations in the time-mean energy budget, *Journal of Climate*, *10*, 1114–1124, 1997.

Callaghan, P., et al., A Hough spectral model for three-dimensional studies of the middle atmosphere, *Journal of the Atmospheric Sciences*, *56*, 1461–1480, 1999.

Cess, R. D., et al., Absorption of solar-radiation by clouds-observations versus models, *Science*, *267*, 496–499, 1995.

Cotton, W. R., and R. A. Anthes, Storm and Cloud Dynamics, Academic Press, 1989.

Goody, R., J. Anderson, and G. North, Testing climate models: An approach, *Bulletin of the American Meteorological Society*, *79*, 2541–2549, 1998.

Hanel, R. A., et al., The Nimbus 4 infrared spectroscopy experiment, I., Calibrated thermal emission spectra, *Journal of Geophysical Research*, *77*, 2629–2641, 1972.

Haskins, R. D., R. Goody, and L. Chen, Radiance covariance and climate models, *Journal of Climate*, *12*, 1409–1422, 1999.

Haskins, R. D., R. M. Goody, and L. Chen, A statistical method for testing a general circulation model with spectrally resolved satellite data, *Journal of Geophysical Research-Atmospheres*, *102*, 16,563–16,581, 1997.

Houghton, J. T., et al., Climate Change 2001: The Scientific Basis, Cambridge University Press, 2001.

Kohler, M., Explicit prediction of ice clouds in general circulation models, *Ph.D. thesis*, University of California, Los Angeles, Los Angeles, 1999.

Leith, C. E., Climate response and fluctuation dissipation, *Journal of Atmospheric Science*, *32*, 2022–2026, 1975.

Madden, R., and P. R. Julian, Detection of a 40–50 day oscillation in the zonal wind in the tropical Pacific, *Journal of Atmospheric Science*, *28*, 702–708, 1971.

Matthews, A. J., Propagation mechanisms for the Madden-Julian Oscillation, *Quarterly Journal of the Royal Meteorological Society*, *126*, 2637–2651, 2000.

Mechoso, C. R., J.-Y. Yu, and A. Arakawa, A coupled GCM pilgrimage: From climate catastrophe to ENSO simulations, in *General Circulation Model Development: Past, present and future*, edited by R. DA, 539–575, Academic Press, 2000.

North, G. R., R. E. Bell, and J. W. Hardin, Fluctuation dissipation in a general circulation model, *Climate Dynamics*, *8*, 259–264, 1993.

Salby, M. L., Climate monitoring from space: Asynoptic sampling considerations, *Journal of Climate*, *2*, 1091–1106, 1989.

Slingo, J. M., et al., Intraseasonal oscillations in 15 Atmospheric General Circulation Models: Results from an AMIP diagnostic subproject, *Climate Dynamics*, *12*, 325–357, 1996.

Wang, J., and G. P. Anderson, Validation of FASCOD3 and MODTRAN3: Comparison of model calculations with interferometer observations from SPECTRE and ITRA, in passive Infrared remote sensing of clouds and the atmosphere II, *Applied Optics*, *35*, 6028–6040, 1996.

X. Huang and Y. L. Yung, Division of Geological and Planetary Sciences, MC 150-21, California Institute of Technology, Pasadena, CA 91125, USA. (yly@gps.caltech.edu)

J. Farrara, Department of Atmospheric Sciences, University of California at Los Angeles, Los Angeles, CA 90095, USA.

S. S. Leroy, Earth and Space Sciences Division, Jet Propulsion Laboratory, Mail Stop 183-335, California Institute of Technology, 4800 Oak Grove Dr., Pasadena, CA 91109, USA.

R. M. Goody, Department of Chemistry and Chemical Biology, Harvard University, Cambridge, MA 02138, USA.